Atomic ordering dependence on growth method in Ge:Si(001) islands: Influence of surface kinetic and thermodynamic interdiffusion mechanisms

A. Malachias,[1,*] M. Stoffel,[2,3] M. Schmidbauer,[4] T. Ü. Schulli,[5] G. Medeiros-Ribeiro,[6] O. G. Schmidt,[3] Rogerio Magalhães-Paniago,[7] and T. H. Metzger[5,8]

[1]*Laboratório Nacional de Luz Síncrotron, CP 6192, CEP 13083-970, Campinas, Brazil*

[2]*Institut Jean Lamour, UMR CNRS 7198, Nancy-Université, BP 239, F-54506 Vandœuvre-lès-Nancy, France*

[3]*Institute for Integrative Nanosciences, IFW Dresden, Helmholtzstr. 20, 01069 Dresden, Germany*

[4]*Leibniz Institut für Kristallzüchtung, Max-Born-Str. 2, D-12489 Berlin, Germany*

[5]*European Synchrotron Research Facility, BP 220, Grenoble, France*

[6]*Hewlett-Packard Laboratories, Palo Alto, California 94304, USA*

[7]*Departamento de Física, Universidade Federal de Minas Gerais, CP 702, 30123-970 Belo Horizonte, MG, Brazil*

[8]*Department of Biomaterials, Max Planck Institute of Colloids and Interfaces, 14424 Potsdam, Germany*

(Received 15 April 2010; revised manuscript received 3 June 2010; published 15 July 2010)

Interdiffusion in self-assembled Ge:Si(001) islands has been explained by models based on either thermodynamic and/or surface kinetic considerations. In order to analyze the relevance of bulk and surface diffusion on the final composition state, we performed a set of controlled x-ray diffraction experiments to study both composition and atomic ordering in Ge/Si(001) islands grown by different methods. Surface diffusion strongly enhances the overall interdiffusion during island growth by solid source molecular beam epitaxy while chemical-vapor-deposited islands are closer to thermodynamic model systems. The growth conditions play a crucial role on the appearance of atomic ordering. In particular, a remarkable correlation between atomic ordering and surface diffusion kinetics is found.

DOI: 10.1103/PhysRevB.82.035307 PACS number(s): 68.65.Hb, 61.05.C−

I. INTRODUCTION

Self-assembled semiconductor islands have gained a tremendous interest over the last years. Novel nanoscale devices based on such islands have been proposed[1] and their use as building blocks for such devices experimentally realized recently.[2] Furthermore, new possible applications in quantum computing[3–5] and spintronics[6,7] were envisaged. The island formation and subsequent evolution has been investigated thoroughly both experimentally and theoretically. Different models based on partially or fully thermodynamic or kinetic considerations have been proposed and are still a matter of controversy.

Most of the studies have concerned Ge:Si(001) islands, that follows Stranski-Krastanow growth mode with only two elements involved. In this specific case, island shapes are well described by thermodynamics[8] while bimodal distributions (for instance) have been tackled by surface kinetics[9,10] and thermal equilibrium arguments.[8,11] Finally, shape transitions observed in ultrahigh vacuum (UHV) growth conditions[12] were found to be associated with strong mass transport effects of surface kinetic origin, referred before as anomalous coarsening.[9,10] Such finding for UHV deposition is in contrast with chemical-vapor-deposition (CVD) studies, in which the range of coexistence for different island shapes, domes and pyramids, is considerably broader.[11] Chemical composition has been addressed in Ge:Si islands by using a variety of techniques such as transmission electron microscopy,[13] anomalous x-ray diffraction,[14] and selective wet chemical etching.[15]

Besides morphological and chemical composition studies, the microscopic organization of Si and Ge atoms after island formation has been addressed by x-ray atomic order studies. It was found that dome-shaped islands in which alloying take place exhibit long-range order with the appearance of superstructure reflections.[16] Although the first study on the subject was unable to elucidate the mechanism that lead to order, it was demonstrated that the atomic arrangement followed the in-plane organization observed in thin films.[17]

In this work we explore chemical composition and atomic order measurements performed using x-ray diffraction techniques to address the relevance of thermodynamic and surface effects to the final state of Ge islands after growth on Si(001). It is found that CVD islands are much closer to model thermodynamic systems while surface kinetics strongly enhances interdiffusion[18] during island growth by molecular-beam epitaxy (MBE). We show here how Ge:Si(001) growth conditions play also a crucial role for the appearance of the recently found atomic order in Ge domes.[16] Such phenomenon exhibits a remarkable correlation with the degree of relevance of surface kinetics on island composition.

II. EXPERIMENTAL

For a thorough investigation on SiGe interdiffusion and on the appearance of spontaneous atomic ordering in Ge:Si uncapped nanostructures, six samples were studied in this work. The first one, grown by liquid-phase epitaxy (LPE), can be considered a reference for stoichiometric alloy islands since $Ge_{0.5}Si_{0.5}$ was nominally deposited on a Si(001) substrate. A second sample, grown by CVD, was obtained by depositing nominally pure Ge via germane precursor (GeH_4) on Si. The other four samples were grown by solid source MBE at different temperatures, also with deposition of a pure Ge nominal coverage. The growth parameters for all samples

TABLE I. List of Ge:Si samples used in this work, with growth parameters, average island dimensions and morphology (Ref. 19).

Sample name	Growth temperature (°C)	Coverage	Growth rate (ML/s)	Island width/height (nm)	Type of island
LPE	600	31.4 ML $Si_{0.5}Ge_{0.5}$ [a]	0.007	81/40	Truncated pyramids
CVD	600	11.2 ML Ge	0.05	32/14	Domes
MBE-a	620	6.7 ML Ge	0.05	87/19	Domes
MBE-b	700	11 ML Ge	0.05	143/36	Domes
MBE-c	750	11 ML Ge	0.05	170/34	Domes
MBE-d	840	6 ML Ge	0.05	338/37	Domes

[a]The monolayer thickness here is considered as 0.1413 nm for Ge, and 0.1385 nm for $Si_{0.5}Ge_{0.5}$.

are summarized in Table I.[19] It must be noticed that LPE islands assume a truncated pyramid geometry with ⟨111⟩ side facets.[20,21] Such morphology indicates that LPE growth takes place very close to bulk thermal equilibrium conditions while MBE- and CVD-grown samples exhibit multifaceted dome islands.[8,9]

It is worth to state at this point that the aim of our work is not to directly compare punctual details of samples grown by different techniques in different machines, but to show how strong changes in interdiffusion and resulting atomic ordering arise from growth conditions, ultimately related to a predominance of bulk thermodynamic or surface kinetic mechanisms. As mentioned before, the apparent contrast found in the literature has been a reason for extensive debate[10] and can be better understood under the general framework illustrated by this work.

The ability of quantitatively depicting strain and chemical composition in Ge islands by anomalous grazing incidence x-ray diffraction (GID) methods[14,22] has continuously developed over the last few years, with several works focusing on the reconstruction of lattice parameter profiles,[22] composition gradients[14,23,24] and ultimately atomic ordering.[16] The GID experiments performed for this work were carried out at the ID01 beamline at the ESRF (Grenoble, France) and at the XRD2 beamline at the LNLS (Campinas, Brazil). In GID geometry the diffraction takes place on atomic planes perpendicular to the Si(001) substrate surface, i.e., the in-plane lattice parameter is probed. All samples were illuminated at a grazing angle of 0.15°, below the critical angle of total external reflection for Si near 11 keV photon energies. This condition establishes a penetration depth of few tens of nanometers, allowing for a partial suppression of the signal from the Si substrate, and a relative enhancement of the signal diffracted by the Ge islands.[14,22]

Chemical composition in Ge:Si nanostructures can be retrieved from reciprocal space data by performing measurements in the vicinity of the Ge *K* edge (11 103 eV). The intensity contrast obtained from measurements in different energies can then be directly correlated with the average Ge content, as depicted in Refs. 14 and 23.

A survey of the real-space reconstruction method using the anomalous-GID measurements performed on sample MBE-b is presented in Fig. 1. Figure 1(a) shows two longitudinal (θ-2θ) scans near the Si(400) reciprocal space posi-

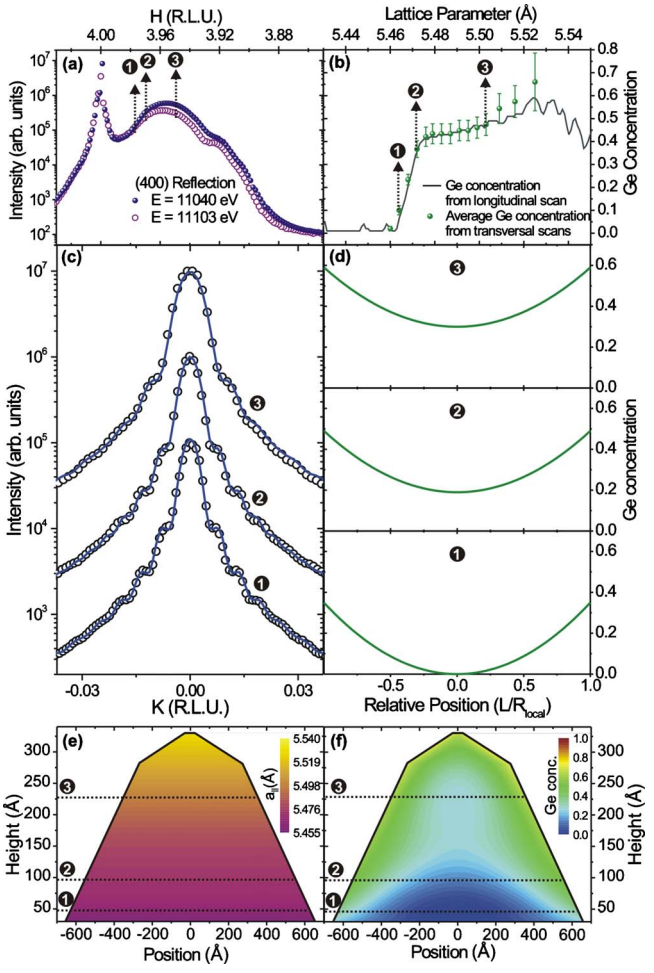

FIG. 1. (Color online) (a) Longitudinal (θ-2θ) scans in the vicinity of the Si(400) reflection for sample MBE-b at two energies: 11 103 eV (Ge *K* edge) and 11 040 eV. (b) The solid line represents the vertical Ge concentration profile obtained from (a) as a function of the local in-plane lattice parameter (Ref. 14). The dots represent laterally averaged local compositions from the analysis of transversal scans. (c) Selected transversal (θ) scans performed at the positions labeled 1, 2, and 3 in (a). The open dots are measured data while the solid lines are fits with a lateral composition model (Ref. 24). (d) Lateral composition profiles used for fitting transversal scans in (c). (e) Local lattice parameter map for MBE-b islands (Ref. 14). (f) Lateral concentration profile map for MBE-b islands.

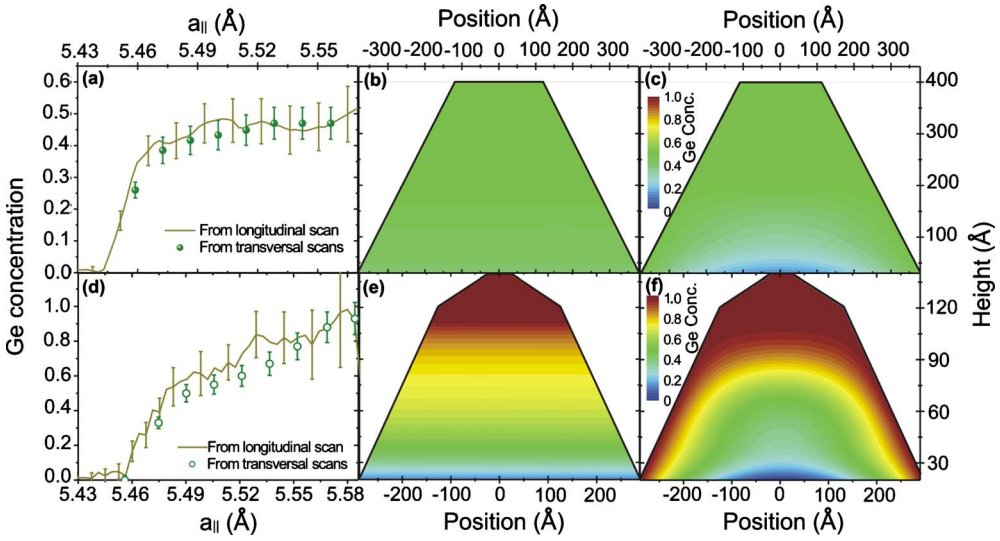

FIG. 2. (Color online) (a) Vertical (solid line) and laterally averaged (dots) Ge concentration profiles extracted from anomalous diffraction measurements on LPE islands. The concentration profiles are graphically represented as a function of height in (b) vertical only and (c) lateral. (d) Ge Vertical and laterally averaged concentration profiles for CVD islands (Ref. 24). These profiles are represented as a function of island height in (e) and (f), respectively.

tion. For both scans it is possible to notice a sharp peak at the $H=4$ position, corresponding to the diffraction from the Si substrate. A broad intensity profile is observed for $H<4$, corresponding to regions with larger lattice parameter, inside the Ge islands.[14] The spanning of such diffracted intensity is a direct indication that a lattice parameter gradient takes place inside Ge domes. For uncapped islands it is known that the scattering intensity closer to the substrate peak is originated from the bottom of the islands while the scattering at the lower H values (large in-plane lattice parameter) comes from partially relaxed regions on the island apexes.[14,22]

By comparing the two measurements presented in Fig. 1(a) obtained at 11040 and 11103eV one observes an intensity reduction for lower values of H which is related to the presence of Ge atoms. Following Refs. 14 and 25, the Ge concentration was extracted, and is represented by the solid line in Fig. 1(b). The concentration profile obtained is still a function of the in-plane lattice parameter. It shows indirectly that the average Ge content at regions of the island with lattice parameter close to bulk Si (island base) reaches almost zero while a SiGe alloy with average 0.5 Ge concentration is found at regions with larger lattice parameter (island top).

In order to match lattice parameter and concentration information from reciprocal space and real space one must perform transversal scans at selected positions of the longitudinal scan of Fig. 1(a). Figure 1(c) shows three scans, corresponding to positions labeled 1, 2, and 3 in Fig. 1(a). The comparison of lateral widths from several transversal scans—obtained fitting the curves with appropriate form factor[22,24]—with atomic force microscopy (AFM) profiles of the statistically average island allows to correlate the height in real space of a region with fixed lattice parameter.[14] A map of lattice parameter distribution for a representative island of the ensemble is then built, as shown in Fig. 1(e).

Transversal (θ) scans also provide information on the lateral concentration profile of the islands. Using a lateral gradient of composition allows to fit each of these scans [solid lines in Fig. 1(c)], extracting the lateral Ge composition.[24] Parabolic concentration profiles used to fit the scans of Fig. 1(c) are shown in Fig. 1(d). The method is finally able to fully depict concentration gradients inside the islands by plotting the profiles of Fig. 1(d) matching the lattice parameter positions in Fig. 1(e). A concentration map including lateral and vertical gradients is then obtained, as shown in Fig. 1(f).[24,26,27] It is important to emphasize that the horizontally averaged lateral composition obtained here is fully consistent with the vertical gradient obtained directly from longitudinal scans,[14] as shown by the solid dots in Fig. 1(b).

III. RESULTS AND DISCUSSION

A. Composition profiles and interdiffusion mechanisms

The composition profile of Fig. 1(f) is in agreement with recent findings using chemical selective etching procedures, as explored in Ref. 15. For such MBE grown samples a considerable Si diffusion is observed in the island bottom with an increasing Ge concentration observed toward the islands facets. However, the Ge concentration at the island surface/interface spans from 0.4 at the island bottom until 0.6 at the island surface.[25] This evidences that alloying takes place at the island bottom, as well as on facets, which are being continuously exposed to an incoming flux of Ge atoms. Such scenario points out the existence of a fast and efficient surface kinetic diffusion component that leads to a pronounced interdiffusion at the facets while the role of bulk diffusion is not significant for the resulting profile.

For LPE and CVD islands the composition profiles shown in Fig. 2 reveal a very different behavior. The average Ge concentration at the top of SiGe LPE islands is found to be 0.48, with a steplike gradient at the island bottom, as shown in Fig. 2(a). By applying only the vertical concentration profile one observes that the Ge content at the island bottom

decreases to about 35% [Fig. 2(b)] while the lateral concentration shows a more localized Si-rich core with only 20% Ge at the island center [Fig. 2(c)]. Similar plateaulike profiles ranging from the LPE island bottom until one third of its height have been obtained before from strain modeling.[20,21] Most of the material inside LPE islands has the nominal alloy content with a reduced interdiffusion from Si atoms from the substrate. This scenario points out that the 50/50 Si-Ge mixture is thermodynamically favorable due to the low enthalpy of mixing. No phase segregation is observed if Figs. 2(b) and 2(c). The Si interdiffusion at the island bottom arises from a slow bulk diffusive process that minimizes the chemical gradient between island and substrate and consists therefore in a thermodynamic driving force for bulk diffusion. Since deposition involves a liquid precursor the process does not allow for quick changes among incoming atoms deposited on the surface and those from the substrate. Thus, with the surface growth front surrounded by the heated precursor stoichiometric alloy liquid, a suppression of any effective surface kinetic diffusion mechanisms is achieved.

For the CVD islands—the smallest of all nanostructures analyzed in this work—a smoother average vertical Ge concentration gradient is obtained [Figs. 2(d) and 2(e)]. However, when such gradient is analyzed by the lateral composition procedure[24] a Ge-rich shell is observed [Fig. 2(f)]. The pronounced composition gradient with a large Si diffusion at the island base is a result from its reduced height and the continuous flux of Ge atoms from the CVD precursor gas. Since a residual passivating hydrogen-rich atmosphere remains at the growth chamber a partial suppression of the kinetic Si interdiffusion mechanisms take place at the island facets (growth front). If the Ge precursor inflow is interrupted, maintaining the growth temperature, the island facets become more Si rich mainly due to bulk diffusion, as shown in Ref. 27 and corroborated by selective chemical etching.[24,28] By introducing a modified atmosphere in the growth chamber Si and/or Ge surface diffusion can be enhanced/suppressed. In particular, H_2 environment strongly reduces Si and Ge surface diffusion, as evidenced experimentally in Ref. 27.

The average vertical composition data extracted from longitudinal scans in anomalous GID is generally a good approach to the local lateral concentration profiles for islands in which the lateral Ge composition gradient is less pronounced, as in MBE and LPE samples. In these islands the local composition is fairly similar in the vertical and three-dimensional profiles. For small islands grown in a surface kinetic limited technique such as CVD the lateral composition gradients are more pronounced and the average vertical concentration profile cannot be regarded as an adequate approximation to the local three-dimensional composition profile. In all cases the vertical averaged and the total Ge concentration obtained by the three-dimensional or by the vertical concentration analysis is the same.

In order to settle the discussion above into a more general and quantitative framework the vertical Ge composition profiles for MBE samples a, c, and d are depicted in Figs. 3(a)–3(c), following the results from Ref. 25. From selective etching experiments in this previous work it was shown that islands are strongly alloyed, with a considerable Si content at

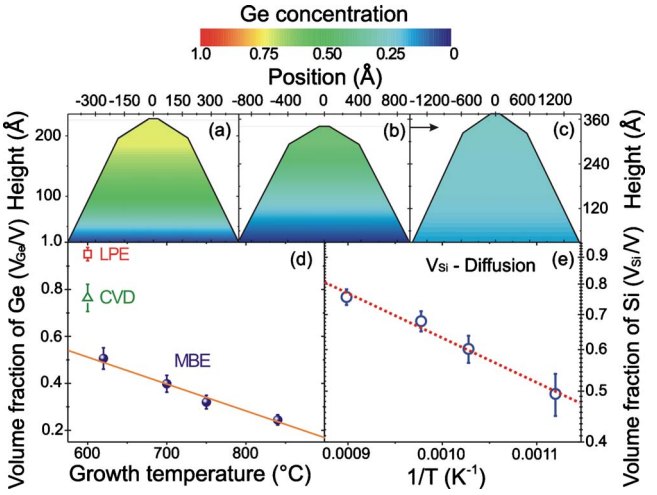

FIG. 3. (Color online) Representation of Ge vertical concentration profiles for islands of samples (a) MBE-a, (b) MBE-c, and (c) MBE-d. The ratio between integrated Ge volume fraction and nominal Ge concentration inside the islands studied in this work is shown in (d). The line plotted across solid dots for MBE islands is a guide to the eyes. An Arrhenius plot for Si volume inside the MBE samples is seen in (e).

their facets, as can be inferred from the vertical composition profiles.[25] By using vertical composition profiles it is possible to explore the volume fraction of alloyed material with respect to nominal deposition values as a function of the growth temperature for all islands. Figure 3(d) shows a representation of the ratio between the measured volume of Ge—or $Si_{0.5}Ge_{0.5}$ in the LPE case—observed in each island and the actual island volume. Figure 3(d) shows that in MBE grown islands a strong deviation with respect to the expected Ge nominal composition is observed for all samples, following a decreasing tendency with respect to temperature. Employing the same evaluation for the LPE sample one observes that the deviation from nominal composition in LPE islands is extremely reduced, which is compatible to a bulk diffusion scenario. For such case the incorporation of Si atoms from the substrate by a slow process results in a much less effective interdiffusion compared to MBE samples. Finally, the CVD grown domes are situated in between MBE and LPE islands, representing a growth condition where both surface or bulk diffusion may take place (depending on residual atmosphere). For these islands the surface kinetic diffusion activity will become clearer by analyzing atomic ordering, discussed in the following paragraphs.

For the MBE samples an Arrhenius plot based on the volume of Si atoms incorporated into the islands can be built, as shown in Fig. 3(e). We obtain an activation energy of 0.073eV for the Si adatoms. Such value is much smaller than the usual activation energies for bulk diffusion, which are on the order of a few electron volt[29] but compatible with kinetic atom step flow energies.[30,31] This kinetic behavior becomes clearer by studying the atomic order of the SiGe-alloyed material inside the islands.

B. Atomic ordering and surface kinetics

SiGe atomic ordering has been observed in thin films and multilayers grown by MBE and CVD,[17] and more recently in

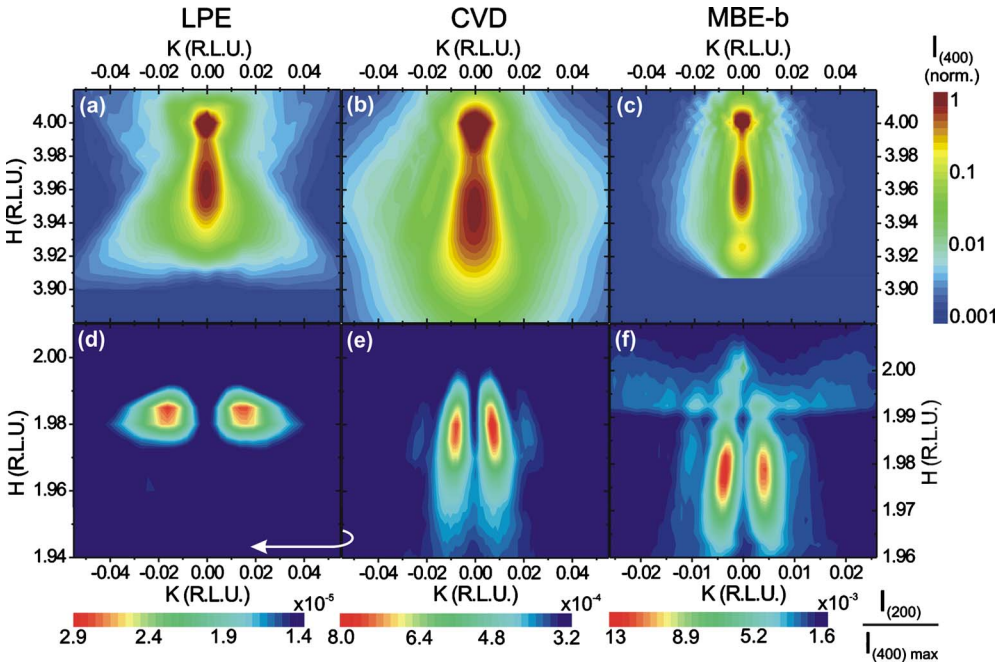

FIG. 4. (Color online) Reciprocal space maps of (400) [(a)–(c)] and (200) reflections [(d)–(f)] for [(a) and (d)] LPE, [(b) and (e)] CVD, and [(c) and (f)] MBE-b samples. The vertical H axis of (d) and (e) are equivalent. Intensity color scales in the (400) maps were normalized to the unit—taken at the island peak position—and to the intensity ratio relative to such maximum at the (200) maps.

Ge:Si(001) islands.[16] In this case Si and Ge atoms are found to be periodically arranged in one (or more) crystallographic axis, giving rise to superstructure reflections that are not observed in elemental pure crystals or disordered alloys. The main evidence of ordering in Ge:Si islands is related to the appearance of nonzero intensity in basis-forbidden Ge/Si reflections such as (200) and (420).[16] For a pure Si or Ge crystal as well as for a completely disordered alloy of both materials the structure factor of these reflections is zero, whereas for an ordered alloy the structure factor of such reflections is proportional to the difference of atomic scattering factors, i.e., $F(200) \propto S^2(f_{Ge}-f_{Si})^2$, where f_{Ge} and f_{Si} are the Ge and Si atomic scattering factors and S is the Bragg-Williams order parameter, discussed in the following paragraphs. Such superstructure reflection was found for all samples studied here. Reciprocal space maps in the vicinity of the Si(400) and (200) reflections are shown in Fig. 4 for selected samples.

The (400) maps of Figs. 4(a) and 4(c) corresponding to the LPE and MBE-b samples, respectively, exhibit diffraction intensity up to $H \sim 3.92$, showing that the alloy material inside both islands relax to approximately the lattice parameter of a $Si_{0.5}Ge_{0.5}$ alloy. Such composition matches the nominal SiGe content of the LPE grown alloy and is in agreement with the maximum Ge concentration of the MBE-b domes obtained in Fig. 1(b). The diffracted intensity at the (400) map obtained for the CVD sample—shown in Fig. 4(b)—spans up to $H \sim 3.87$, indicating that the CVD islands have a higher Ge content if compared to the LPE and MBE-b samples. The intensity data in all (400) reflection maps was normalized to unity at the island peak position of each sample.

On the (200) maps of Figs. 4(d)–4(f) one observes a double-peak feature along the K (transversal) direction. As reported in previous works intensity from ordered alloys in SiGe islands exhibit a particular reciprocal space imprint with a two-peak structure along the transversal (K) direction, generated by the existence of antiphase boundaries.[16] It is worth to compare the extent of the (200) intensity maps along the H direction relative to the extent of the (400) maps. For the LPE sample the (200) intensity [Fig. 4(d)] spans to a minimum H value of 1.975 while the (400) map [Fig. 4(a)] exhibits considerable diffracted intensity up to $H \sim 3.905$ (or 2×1.952). It is expected, therefore, that ordered alloys can be found only in regions of the islands where the local lattice parameter correspond to strained conditions. For the CVD sample, the reciprocal space extent of the (200) map reaches $H \sim 1.95$, still limited with respect to the extent of the (400) intensity, that reaches $H \sim 3.87$ (or 2×1.935). Finally, for the MBE-b sample the (200) intensity spans until $H \sim 1.96$ a value comparable to the extent of the (400) reflection $H \sim 3.91$ (2×1.955).

The quantification of the degree of order in the alloys of the samples studied here can be drawn by evaluating the intensity ratio between the (200) superstructure reflection and the (400) fundamental reflection. This ratio is shown in the different color scales of Figs. 4(d)–4(f), where the intensity normalization for each map was performed with respect to the maximum of diffraction intensity in the island position of (400) maps. Since Si, Ge, and SiGe alloy crystals have the diamond unit cell the Bragg-Williams order parameter S can be obtained from the ratio of intensities[32] as

$$\frac{I_{(200)}}{I_{(400)}} = \frac{S^2(f_{Ge}-f_{Si})^2}{4(\langle f_{GeSi}\rangle)^2}, \tag{1}$$

where f_{Ge} and f_{Si} are the Ge and Si atomic scattering factors, respectively, and $\langle f_{GeSi}\rangle = C_{Ge}f_{Ge} + C_{Si}f_{Si}$ is the local effective

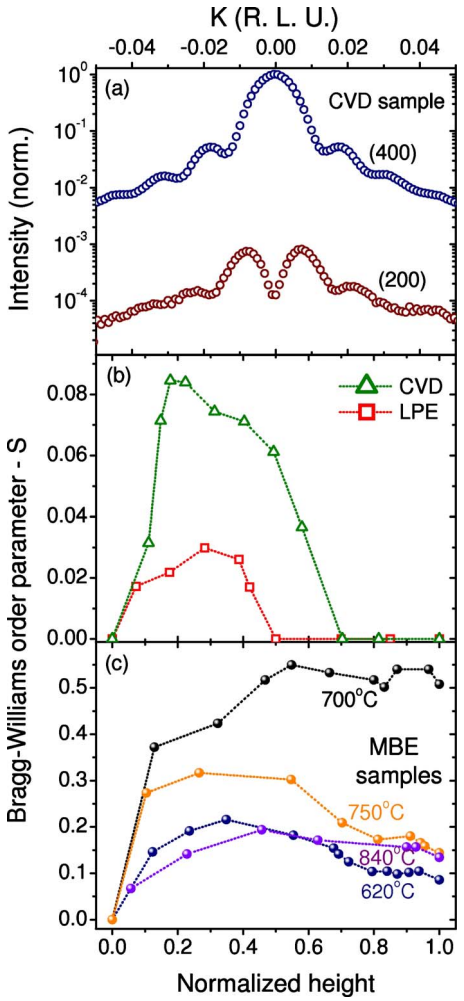

FIG. 5. (Color online) (a) Transversal scans at $H=3.95$ and $H=1.975$ for the (400) and (200) reciprocal space maps, respectively, measured for the CVD sample. (b) Bragg-Williams order parameter S as a function of the normalized height for LPE and CVD islands. (c) Values of S for all MBE samples measured in this work.

atomic scattering factor for a SiGe alloy. Typical S values range from zero to unity as the superstructure reflection is measured from a fully disordered alloy ($S=0$) until a completely ordered crystal ($S=1$).[16,32]

All reciprocal space maps of Fig. 4 are composed of transversal scans. Transversal scans for the CVD islands obtained from Fig. 4(b) at $H=3.95$ and from Fig. 4(e) at $H=1.975$ are depicted in Fig. 5(a). For each transversal scan in a (400) map an equivalent transversal scan was performed to build the (200) map, allowing to integrate the diffracted intensity at each reciprocal space position along the map and evaluate the local order parameter on each sample. Finally, in order to express S as a function of the island height the procedure adopted is an extension of the procedure employed to build the maps of Fig. 1(e). Each transversal cut from the (400) map represents a local strain status inside the island that can be directly related to a region in real space by the lateral dimension extracted from the width of the transversal scan. Such width is then compared to a real space AFM profile and the height above the substrate for an isolattice parameter region obtained. We assume, therefore, that a region with a given lattice parameter in the (200) map is located at the same height from the substrate in the island as a region assigned to the equivalent strain status in the (400) map. This assumption is valid since a monotonic vertical lattice parameter relaxation takes place in all islands and such vertical gradient is much more pronounced than possible lateral strain gradients inside these nanostructures.[22] The lateral position of the ordered domains inside Ge:Si islands could not be addressed by our model.[16] For this reason we follow our analysis exploring the vertical dependence of S.

Applying Eq. (1) for the integrated area of transversal scans at (400) and (200) maps one can obtain S and express it as a function of the island height. Since islands analyzed in this work have different heights a quick visualization procedure of the order degree in each case can be performed by plotting S as a function of the normalized island height, assumed to be unity at the apex of each island. Figures 5(b) and 5(c) show these results for the LPE, CVD, and all MBE islands. As shown in Fig. 4, (200) maps for all samples exhibit a very low intensity at the vicinity of the Si reciprocal space position, in contrast to a strong substrate peak at the (400) reflection. Since this condition is also related to Si-rich regions at the islands basis, the evaluation of S at such reciprocal space positions lead to very small values. For this reason graphs of Figs. 5(b) and 5(c) show $S=0$ for all island basis. Such values are reasonable for MBE samples where the Si diffusion is more severe at the islands bottom but certainly deviate from the expected in the LPE and CVD cases. S values obtained for corresponding positions in the (400) map where the island diffraction signal is predominant ($H<3.99$) are accurate.

A first look to the S profile obtained for the LPE sample shows that a very reduced order is found in these alloyed islands. By evaluating the size of ordered regions by the procedure of Ref. 16 one finds an average domain size of 45 Å. Since the diffracted intensity from a superstructure reflection is proportional to the volume of ordered material, independently from the number of existing ordered domains[32] such result indicates that a very small amount of material relative to the total islands volume is ordered from the LPE growth. In this system, in which the alloying process is much closer to expected thermodynamic behavior, the enthalpy of mixing for an ordered alloy is extremely high[33] and mixing entropy is maximized, leading to an almost fully random SiGe alloy. The ordered regions are mainly present at the island bottom part where the local strain has a maximum value. As shown in the S map of Fig. 6(a) the observed ordering is roughly limited to one-third of the island height.

CVD domes exhibit larger S values if compared to the LPE $Si_{0.5}Ge_{0.5}$ truncated pyramid islands. This result is rather unexpected for islands that have grown from the deposition of a pure Ge precursor (GeH_4). It is clear, therefore, that the incorporation of Si atoms by bulk and/or surface kinetic diffusion is responsible for generating the necessary stoichiometric conditions for alloying and ordering. As pointed out in Ref. 24 the incoming Ge atoms play a crucial role to the final concentration profile observed in CVD islands by producing a Ge-rich outer cap at the island, indicating that sur-

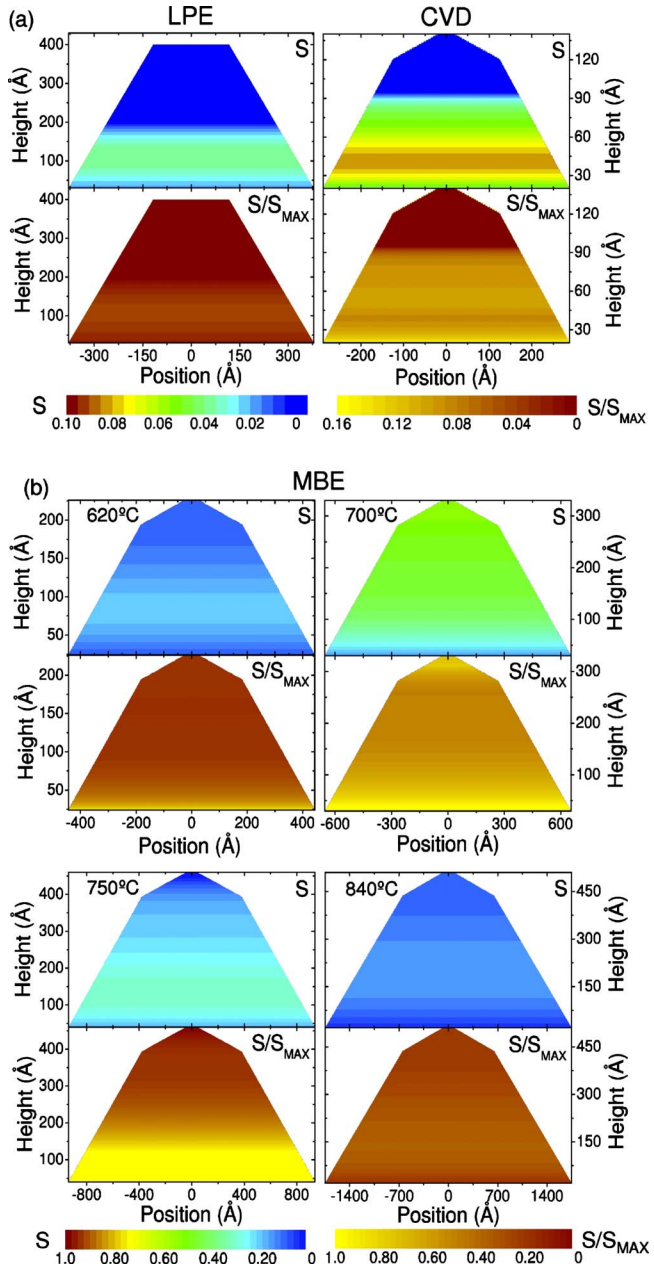

FIG. 6. (Color online) (a) Representation of Bragg-Williams order parameter S and the S/S_{max} ratio (see text) for LPE and CVD islands. The color scale for these maps is the same for both samples. (b) Maps of S and S/S_{max} for all MBE islands. The color scales for these four samples are shown in the bottom of the figure.

face kinetic diffusion—that would be responsible for alloying at the island facets—is reduced with respect to MBE samples [as also discussed for the results of Fig. 3(d)]. CVD islands behave, therefore, as systems in a condition much closer to thermodynamic equilibrium,[8] due to partial hydrogen passivation of the surface, but with a non-negligible influence from surface kinetic phenomena. The proximity to thermal equilibrium leads to a pyramid-to-dome transition in which anomalous coarsening is much less effective than in MBE growth. Such transitions are related to the appearance of large island facets that differ from the expected equilibrium ⟨111⟩ or ⟨100⟩ Wulff construction symmetry, allowing for surface reconstructions at the ⟨113⟩ and ⟨15 3 23⟩ facets that may be crucial for an increase in surface atomic mobility at multifaceted dome islands. These facets are steeper than those of shallow ⟨105⟩ faceted pyramids also obtained by MBE and/or CVD and will be hereafter referred as "steeper facets." The resulting composition profile exhibits a vertically limited Si interdiffusion at the island center as a result from the combination of the slow Si bulk diffusion process and the continuous Ge atom flux. However, the incorporation of Si atoms is much stronger laterally—although a thin Ge-rich cap is still present—indicating that some small degree of surface Si-Ge diffusion takes place at the domes steeper facets. If Ge deposition is interrupted the steeper facets become more Si rich while the composition evolution at the island center is slower. This indicates the existence of a surface kinetic alloying mechanism for this growth method.[27] From the CVD S profile of Fig. 5(b), represented in the CVD S map of Fig. 6(a) one observes that ordered alloying is limited to the regions of the islands with steeper facets. This is also in agreement with the vertical extent of the Ge-pure region at the island top of Fig. 2(f). The average ordered domain size was found to be of 75 Å for CVD islands.

Finally, all MBE islands measured here exhibit S values much larger than for samples grown by other methods. From Fig. 5(c) one observes that S reaches considerably high values, having a maximum around 40% of the island height, and lower S values closer to the island top (except for sample MBE-b). Islands grown at 700 °C have shown an exceptionally high value of S, which results from matching the center of the temperature window in which order is more favorable with the conditions that provide a 50% Ge content into the islands. The nonvanishing S behavior for this growth temperature can be explained by the reciprocal space broadening of both (200) and (400) profiles along H due to finite size of isolattice parameter regions and ordered domains. Most notably for the MBE-b sample, for H values of transversal scans that correspond to the island apex at the (400) reflection, there is always diffracted intensity above the background at the equivalent transversal scan at the (200) map. For temperatures higher than 700 °C entropy of mixing increases, leading to lower values of S as shown in Fig. 5(c). Although islands may not be completely ordered from bottom to apex the values shown in Fig. 5(d) are more accurate at the middle height of these structures.

The difference in almost 1 order of magnitude for S values in the MBE islands with respect to LPE alloy islands is in clear contrast with the optimum composition for ordering since MBE islands exhibit stronger composition gradients. Such condition implies the existence of regions in which the stoichiometry deviates from 50/50. One can assume, therefore, that the mixing entropy is maximized in the LPE alloy system, as a tendency from thermodynamic equilibrium behavior, while another mechanism is responsible for the larger ordering in the MBE islands.

An alternative way to compare SiGe ordering in all islands can be established by evaluating the ratio S/S_{max}, where S_{max} is the maximum value of S that can be reached for a given local Ge/Si composition. S_{max} can be defined as $S_{max}=1-|C_{Ge}-C_{Si}|$, where C_{Ge} and C_{Si} are the local Ge and Si concentrations. This definition is in agreement with the

definition of S,[32] and leads to $S_{max}=1$ for $C_{Ge}=C_{Si}=0.5$ and $S_{max}=0$ for a pure material. Therefore, using the S/S_{max} ratio it is possible to evaluate in which regions of the islands atomic order is more effective. Similar to the behavior of S, S/S_{max} tends to be inaccurate at the island basis, where small finite S values are found in very Si-rich regions. For island regions where C_{Ge} is larger than 0.1 the S/S_{max} ratio is more accurate and also indicates that order is more effective at the region of the islands where steeper facets are found.

IV. CONCLUSION

As discussed before, surface kinetic diffusion is strongly related to the larger incorporation of Si atoms in MBE growth in comparison with CVD and LPE. In this case, the surface reconstruction that takes place at the island facets is probably responsible for alloying Si and Ge atoms during the deposition process. The larger mobility obtained by UHV-MBE growth can, therefore, generate conditions that favor Si and Ge adatom bonding at the steeper island facets. Ordering would be, then, a result of alloying at the ⟨113⟩ and ⟨15 3 23⟩ dome facets. An indication of this facet mediated mechanism is observed by the presence of maximum S on the equivalent island height for these facets observed for the MBE and CVD samples in Figs. 6(a) and 6(b).

In conclusion, Ge:Si atomic ordering was evidenced in dome-faceted islands, with a remarkably strong signal from MBE-grown samples. Although the precise mechanism of ordering remains unclear we have shown that surface diffusion plays a key role in this phenomenon by comparing different growth methods. The poor degree of ordering measured for an alloyed LPE sample suggests that surface reconstruction at the domes steeper facets is the key for atomic ordering. We hence suggest that *in situ* scanning tunneling microscopy experiments at islands steeper facets (on the edge of a substrate) can shed some more light into the kinetic mixing that takes place in these regions. Although such kind of experiment cannot distinguish among Si and Ge atoms, it can surely provide the configuration of the surface atoms at the facets. The exact knowledge of such surface reconstruction and its energetic balance in dome islands will certainly improve the understanding of both kinetic diffusion and atomic ordering mechanisms in this system. CVD and MBE ⟨105⟩ faceted pyramids were also measured for this work and have shown no sign of ordering, corroborating the influence of dome facets on GeSi order. By assuming that steeper facets are responsible for atomic ordering one can explain the fourfold symmetry obtained when observing similar antiphase boundary diffraction profiles in all ⟨100⟩ orientations used to measure in-plane (200) reflections. In particular, measurements of the superstructure (200) reflection for Ge:Si islands have shown to be able to indicate and quantify relatively the existence of kinetic diffusion behavior during growth. Finally, the atomic order previously observed for the wetting layer formed on the ⟨001⟩ Si substrate surface is very reduced with respect to the order obtained in Ge domes, suggesting that different mechanisms are responsible for each of these phenomena.[34]

ACKNOWLEDGMENTS

This work was supported by the Brazilian agencies CAPES and CNPq.

*Present address: Laboratório Nacional de Luz Síncrotron C.P. 6192–Campinas, Brazil; amalachias@lnls.br

[1] G. S. Kar, S. Kiravittaya, U. Denker, B. Y. Nguyen, and O. G. Schmidt, Appl. Phys. Lett. **88**, 253108 (2006).
[2] G. Katsaros, P. Spathis, M. Stoffel, F. Fournel, M. Mongillo, V. Bouchiat, F. Lefloch, A. Rastelli, O. G. Schmidt, and S. De Franceschi, Nat. Nanotechnol. **5**, 458 (2010).
[3] M. Nomura, N. Kumagai, S. Iwamoto, Y. Ota, and Y. Arakawa, Nat. Phys. **6**, 279 (2010).
[4] H. Oka, P. A. Ignatiev, S. Wedekind, G. Rodary, L. Niebergall, V. Stepanyuk, D. Sander, and J. Kirschner, Science **327**, 843 (2010).
[5] L. Wang, A. Rastelli, S. Kiravittaya, M. Benyoucef, and O. G. Schmidt, Adv. Mater. **21**, 2601 (2009).
[6] A. F. Zinovieva, A. V. Dvurechenskii, N. P. Stepina, A. S. Deryabin, A. I. Nikiforov, R. M. Rubinger, N. A. Sobolev, J. P. Leitão, and M. C. Carmo, Phys. Rev. B **77**, 115319 (2008).
[7] F. Lipps, F. Pezzoli, M. Stoffel, C. Deneke, J. Thomas, A. Rastelli, V. Kataev, O. G. Schmidt, and B. Büchner, Phys. Rev. B **81**, 125312 (2010).
[8] G. Medeiros-Ribeiro, A. M. Bratkovski, T. I. Kamins, D. A. A. Ohlberg, and R. S. Williams, Science **279**, 353 (1998).
[9] F. M. Ross, J. Tersoff, and R. M. Tromp, Phys. Rev. Lett. **80**, 984 (1998).
[10] A. Rastelli, M. Stoffel, J. Tersoff, G. S. Kar, and O. G. Schmidt, Phys. Rev. Lett. **95**, 026103 (2005).
[11] R. E. Rudd, G. A. Briggs, A. P. Sutton, G. Medeiros-Ribeiro, and R. S. Williams, Phys. Rev. Lett. **90**, 146101 (2003).
[12] F. Montalenti, P. Raiteri, D. B. Migas, H. von Känel, A. Rastelli, C. Manzano, G. Costantini, U. Denker, O. G. Schmidt, K. Kern, and L. Miglio, Phys. Rev. Lett. **93**, 216102 (2004).
[13] X. Z. Liao, J. Zou, D. J. H. Cockayne, J. Wan, Z. M. Jiang, G. Jin, and K. L. Wang, Phys. Rev. B **65**, 153306 (2002).
[14] R. Magalhães-Paniago, G. Medeiros-Ribeiro, A. Malachias, S. Kycia, T. I. Kamins, and R. Stan Williams, Phys. Rev. B **66**, 245312 (2002).
[15] A. Rastelli, M. Stoffel, A. Malachias, T. Merdzhanova, G. Katsaros, K. Kern, T. H. Metzger, and O. G. Schmidt, Nano Lett. **8**, 1404 (2008).
[16] A. Malachias, T. Ü. Schülli, G. Medeiros-Ribeiro, L. G. Cançado, M. Stoffel, O. G. Schmidt, T. H. Metzger, and R. Magalhães-Paniago, Phys. Rev. B **72**, 165315 (2005).
[17] J. Z. Tischler, J. D. Budai, D. E. Jesson, G. Eres, P. Zscack, J. M. Baribeau, and D. C. Houghton, Phys. Rev. B **51**, 10947 (1995).
[18] Here the term interdiffusion refers to any general mixing mechanism. In the manuscript text the terms "surface diffusion" and "bulk diffusion" were used to refer specifically to these mechanisms, when they apply.

[19] The main type of island for all MBE samples studied here are dome-shaped and barn-shaped, both presenting ⟨113⟩ and ⟨15 3 23⟩ facets. In order to keep consistence with Ref. 25, in which the composition in these islands was firstly analyzed, the island type for MBE samples will be referred here as domes. A very reduced population of superdomes (<5%), not statistically significant to influence the diffraction profiles, can be found in these samples.

[20] Th. Wiebach, M. Schmidbauer, M. Hanke, H. Raidt, R. Köhler, and H. Wawra, Phys. Rev. B **61**, 5571 (2000).

[21] M. Hanke, M. Schmidbauer, D. Grigoriev, H. Raidt, P. Schäfer, R. Köhler, A.-K. Gerlitzke, and H. Wawra, Phys. Rev. B **69**, 075317 (2004).

[22] I. Kegel, T. H. Metzger, A. Lorke, J. Peisl, J. Stangl, G. Bauer, K. Nordlund, W. V. Schoenfeld, and P. M. Petroff, Phys. Rev. B **63**, 035318 (2001).

[23] T. U. Schülli, J. Stangl, Z. Zhong, R. T. Lechner, M. Sztucki, T. H. Metzger, and G. Bauer, Phys. Rev. Lett. **90**, 066105 (2003).

[24] A. Malachias, S. Kycia, G. Medeiros-Ribeiro, R. Magalhães-Paniago, T. I. Kamins, and R. S. Williams, Phys. Rev. Lett. **91**, 176101 (2003).

[25] T. U. Schülli, M. Stoffel, A. Hesse, J. Stangl, R. T. Lechner, E. Wintersberger, M. Sztucki, T. H. Metzger, O. G. Schmidt, and G. Bauer, Phys. Rev. B **71**, 035326 (2005).

[26] G. Medeiros-Ribeiro, A. Malachias, S. Kycia, R. Magalhães-Paniago, T. I. Kamins, and R. Stanley Williams, Appl. Phys. A: Mater. Sci. Process. **80**, 1211 (2005).

[27] M. S. Leite, A. Malachias, S. W. Kycia, T. I. Kamins, R. S. Williams, and G. Medeiros-Ribeiro, Phys. Rev. Lett. **100**, 226101 (2008).

[28] M. S. Leite, G. Medeiros-Ribeiro, T. I. Kamins, and R. S. Williams, Phys. Rev. Lett. **98**, 165901 (2007).

[29] M. Meduna, J. Novak, G. Bauer, V. Holy, C. V. Falub, S. Tsujino, and D. Grutzmacher, Semicond. Sci. Technol. **22**, 447 (2007).

[30] J. B. Hannon, M. Copel, R. Stumpf, M. C. Reuter, and R. Tromp, Phys. Rev. Lett. **92**, 216104 (2004).

[31] D. E. Jesson, S. J. Pennycook, and J.-M. Baribeau, Phys. Rev. Lett. **66**, 750 (1991).

[32] B. E. Warren, *X-Ray Diffraction* (Dover, New York, 1969).

[33] J. E. Bernard and A. Zunger, Phys. Rev. B **44**, 1663 (1991).

[34] A. Malachias, T. H. Metzger, M. Stoffel, O. G. Schmidt, and V. Holy, Thin Solid Films **515**, 5587 (2007).